IN SEARCH OF SUBSURFACE OCEANS WITHIN THE MOONS OF URANUS.

C.J. Cochrane[1], T.A. Nordheim [1], S.D. Vance[1], M. Styczinski[2], K. Soderlund[3], C. M. Elder[1], E. J. Leonard[1], R. J. Cartwright[4], C. B. Beddingfield[4,5], L. H. Regoli[6], N. Gomez-Perez[7]. [1]Jet Propulsion Laboratory, California Institute of Technology (corey.j.cochrane@jpl.nasa.gov), [2]University of Washington, [3]University of Texas at Austin, Institute for Geophysics, [4]SETI Institute, [5]NASA Ames Research Center, [6]John Hopkins University Applied Physics Laboratory, [7]British Geologic Survey.

Introduction: Magnetic induction has been a valuable mechanism for probing the interior of planetary bodies in search of subsurface oceans within our solar system, the prime examples being the Galileo magnetometer investigation of oceans on Europa and Callisto [1]. The major Uranian moons are also well suited for a magnetic induction study as each are exposed to a strong time-varying magnetic field due to the tilt of Uranus' magnetic axis with respect to its spin axis, in addition to the slight eccentricity and inclination of the moons [2,3]. External time varying magnetic fields will induce currents within any conductive layers of the moon, which results in the generation of a secondary magnetic moment that is roughly proportional to and in the opposite direction of the primary field. The strength and phase-delay of the secondary field will depend on interior properties of the moon (e.g. thickness and conductivity of various layers) making it ideal for magnetic sounding of potential ocean worlds. Based on geological features, images of the Uranian satellites collected by Voyager 2 suggest that these moons could have harbored subsurface oceans earlier in their histories and could possibly still host them today [4,5,6]

In this work, we assess the spectral content of the magnetic environment experienced by the moons from the Uranian magnetic field (see Fig 1) to determine the specific frequencies at which each of these moons can be probed and the anticipated amplitude and phase delay expected in their induction responses. We also present preliminary interior structures for Ariel and Miranda (see Fig 2) and discuss the possibility of motional induction through ocean circulations. This work provides insight into potential future mission concepts and magnetometer specifications.

Methods & Results: For a subset of models, it is instructive to examine the full spectral response of complex magnetic induction [7]. By analogy to Enceladus, we examine two interior models for Miranda spanning a plausible range of global ice thicknesses. We specify a seawater composition (35 ppt salinity) and compute self-consistent structures using TEOS-10 [8] with the PlanetProfile package [9]. The self-consistent models have ocean (ice) thicknesses of 25 (76) km and 85 (14) km, with mean conductivities of 2.7 S/m. The corresponding amplitude and phase curves (Fig. 3), computed for depth-dependent conductivities, match the magnetic contours in Fig 2. Although a strong signal exists at the 1004-hr period (the beat frequency associated with the very small difference of the synodic and orbital periods), it seems likely that such a signal will not induce a strong induction response for plausible oceans in Miranda due to the attenuation in amplitude expected at this frequency.

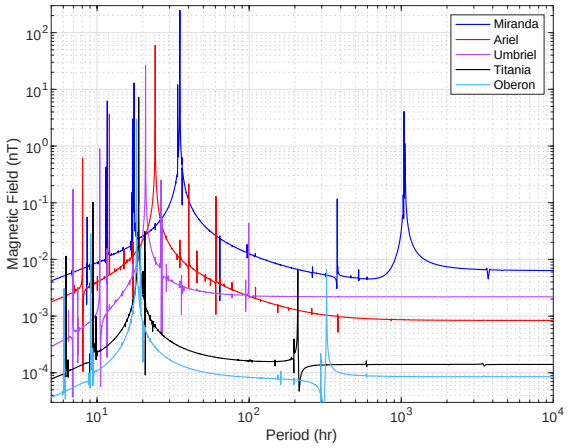

Figure 1: Magnitude of Uranus' magnetic field evaluated at the orbital position of its five major moons as a function of frequency.

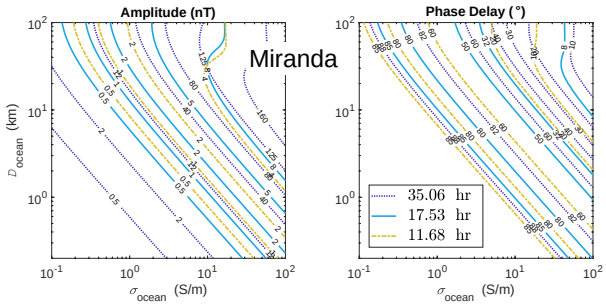

Figure 2: Contour plots illustrating magnetic moment (based on planetocentric B_y) and phase delay of the (blue dots) Uranus synodic, (cyan) 2nd harmonic, and (yellow dot-dash) 3rd harmonic periods for Miranda, assuming a 3-layer shell model (20-km non-conducting ice shell, conducting ocean layer, non-conductive interior).

The full waveform response combining phase and amplitude information can be inspected by plotting real and imaginary parts of the complex wave form to examine the internal induced responses arising in phase (Re) and out of phase (Im) with the external field of Uranus. Figure 4 illustrates the responses weighted by the strength in the field at the periods noted in Figure 3.

In contrast with the analogous set of signals recently examined for Jupiter's ocean moons, Miranda's strongest signal (at the synodic period of Uranus) is actually slightly longer than the orbital period. Additional strong oscillations occur at the 2nd and 3rd harmonics of the synodic period. All three oscillations create signals larger than 1 nT, even for the smaller ocean, as also reported by [Weiss2020AGU].

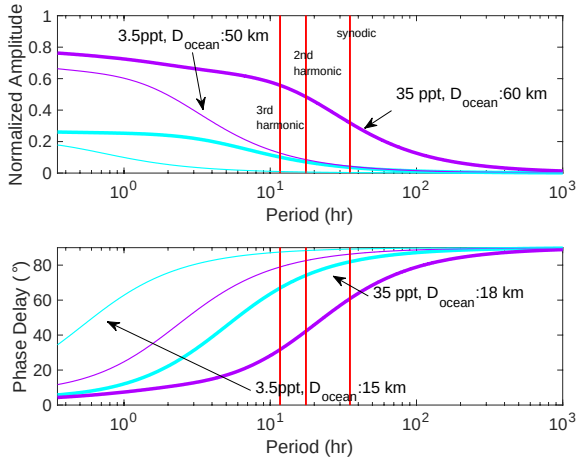

Figure 3. Spectral amplitude and phase response for two plausible model seawater oceans in Miranda. Vertical lines demarcate the synodic period and its strong harmonics.

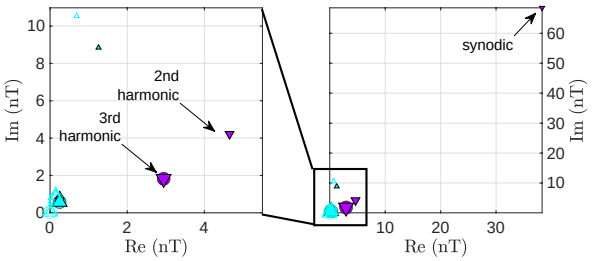

Figure 4. Complex response function parameters for Miranda at the synodic period and its strong harmonics.

As little is known about the properties of the Uranian moons, a wide variety of possible candidate interiors is possible for each body. Detection of oceans within the moons, by analyzing future measurements, may be made more difficult by possible asymmetries in the oceans [10]. An analogy may be made by considering Callisto, for which there is evidence of a strong day–night asymmetry in the ionosphere [11] that may yet account for much of the observed induction signal [12]. Similarly, Enceladus hosts a marked hemispheric asymmetry that may be an expected outcome for smaller moons like Miranda. Applying recent advances in theoretical techniques (e.g., [10]), we consider a variety of asymmetric conductivity structures that may be present in the ionospheres and oceans of the Uranian moons, such as a tidal bulge or day–night dichotomy. The impact of these asymmetric features are quantified by comparison to symmetric models. In this way, we determine the degree of uncertainty in ocean characterization and set detection thresholds for candidate oceans.

Finally, we also assess whether fluid motions within the oceans themselves (e.g., due to convection, mechanical driving, and/or electromagnetic forcing) may generate induced magnetic fields that would add uncertainties to magnetic field inversion calculations for ocean conductivity and thickness. Following the approach developed in [9], magnetic fields generated by such motional induction can be estimated as $b \sim \mu_0 \sigma U D B_0$ where μ_0 is the magnetic constant, σ is electrical conductivity, U is characteristic flow speed, D is ocean theld measured at the satellite. At the surface, the induced magnetic field will be a factor of $(r_{satelite}/r_{ocean})^{l+2}$ times weaker, where l is spherical harmonic degree. An induced dipolar $l = 1$ magnetic field of $b = 1\ nT$ nT at the surface would then require flow speeds of $U \sim 1$ cm/s ($U \sim 10$ cm/s) for the thick (thin) ocean scenario for Miranda, which are comparable to or stronger than convective flow speeds estimated for Enceladus [14].

Discussion: Magnetic induction is a powerful mechanism that can be used to detect potential oceans within the major moons of Uranus. Because of the strong and dynamic environment in which they reside, single-pass ocean detection may even be possible. Beyond a new mission to the Uranian system, material properties and detailed motional induction modeling are needed to characterize the oceans' compositions and thicknesses.

Acknowledgments: Funded by the JPL Strategic Research & Technology Development program and Icy Worlds project (13-13NAI7_2-0024).

References:

[1] Zimmer, C., Khurana, K.K., Kivelson, M.G., (2000). Icarus, 147, 329–347. [2] Connerney, J.E.P., Acuna, M.H., Ness, N.F., (1987) JRG 92, 15329-15336. [3] Herbert, F. (2009), JGR., 114, A11206, [4] Hussman et al., 2006 (doi:10.1016/j.icarus.2006. 06.005). [5] Cartwright et al., 2020 (doi:10.3847/20418213/aba27f). [6] Schenk et al., 2020 (doi: 10.1098/rsta.2020.0102). [7] Vance, S. D. et al. (2018) *JGR-Planets*, 123,180-205, doi:10.1002/2017JE005341. [8] McDougall, T. J. et al. (2011). *SCOR/IAPSO WG*, 127, 1–28. [9] Vance, S. D. et al. (2021). *JGR-Planets*, in press. [10] Styczinski, M. J. and Harnett, E. M., (2021). Icarus, 354, 114020. [11] Hartkorn, O., Saur, J. Strobel, D. F., (2017). Icarus, 282, 237–259. [12] Liuzzo, L. et al., (2017). JGR-SP, 122 (7), 7364–7386. [13] Kang, W. et al. Aug 2020 preprint. arXiv:2008.03764. [14] Soderlund, K. M. (2019) GRL, 46(15), 8700-8710.